Characteristics of Chemical Solutes and Mineral Dust in Ice of the Ablation Area of a Glacier in Tien Shan Mountains, Central Asia

Yunjie Chen[1]*, Nozomu Takeuchi[1], Feiteng Wang[2] and Zhongqin Li[2]

[1]Department of Earth Sciences, Graduate School of Science, Chiba University, Chiba, Japan, [2]State Key Laboratory of Cryospheric Sciences/Tien Shan Glaciological Station, Northwest Institute of Eco-Environment and Resources, Chinese Academy of Sciences, Lanzhou, China

Diverse microbial communities live on glacial surfaces, with abundances and diversities dictated by the chemical and physical conditions of the supraglacial environment. Chemical solutes and mineral dust on glacial surfaces are generally derived from the atmosphere as aerosols, but they can also be supplied from glacial ice. In this study, a 56-m ice core from the ablation area of a mountain glacier in the Tien Shan Mountains of Central Asia was analyzed to characterize the chemical solutes and mineral dust in glacial ice. Soluble chemical ion and mineral dust analysis in the ice core showed that their concentrations varied with depth. The most dominant ion was Ca^{2+} (mean: 79.8 µEq L^{-1}), followed by Cl^-, SO_4^{2-}, NH_4^+, and NO_3^-. The mean dust concentration in the glacial ice was 2.5×10^5 number ml^{-1}. Chemical solute and mineral dust concentrations in the samples indicate that melting glacial ice could potentially affect supraglacial conditions. The annual fluxes of the major ions outcropping from glacial ice were estimated based on their concentrations and the observed melt rate of the ice surface. Consequently, they were comparable to or higher than those from the atmosphere. The mean mass flux of mineral dust from glacial ice was greater than that from the atmosphere. Our results showed that glacial ice supplies chemical solutes and mineral dust to the supraglacial environment and that changing melting rates of glacial ice would affect the chemical conditions on the glacier surface and the growth of photoautotrophs on the ablating ice surface.

Keywords: glacial ice, ice core, supraglacial environments, mineral dust, soluble ions, outcropping flux

1 INTRODUCTION

The mass loss of glaciers has been reported globally since the 20th century (Haeberli et al., 2000; Barry, 2006; Li et al., 2011b), and recent studies have shown that the shrinkage of glaciers is caused not only by global warming but also by albedo reduction of glacier surfaces (Li et al., 2011a). Albedo reduction of glacier surfaces allows more shortwave radiation to be absorbed on the surface and accelerates ice and snow melting. One of the major factors that decrease albedo is light-absorbing impurities on the ice or snow surface (Wiscombe and Warren, 1980). The major light-absorbing impurities on the glacier surface are black carbon (BC), derived from fossil fuel combustion and biomass burning (Bond et al., 2013), and mineral dust, which is wind-blown dust derived from the

crustal surface via the atmosphere (Bøggild et al., 2010). Furthermore, recent studies have revealed that organic matter produced by snow- or ice-inhabiting microbes are also light-absorbing impurities (Takeuchi et al., 2001a, 2001b, 2002, 2005, 2006, 2010; Takeuchi, 2002; Takeuchi and Li, 2008).

Cold-adapted microbes, including bacteria, cyanobacteria, algae, and fungi, are distributed on glaciers worldwide and actively grow during the melting season (e.g., Langford et al., 2010; Segawa et al., 2014; Uetake et al., 2016). Photoautotrophs, such as cyanobacteria and algae, can photosynthetically produce organic matter and are primary producers in glacial ecosystems (Hoham and Remias, 2020). As such, these photoautotrophs can sustain heterotrophic microorganisms on glaciers, such as bacteria, rotifers, and tardigrades (e.g., Zawierucha et al., 2015; 2021).

Glacial microbes often form aggregates with mineral particles and organic matter, called cryoconite, and can reduce the albedo of glacier surfaces (Cook et al., 2016). The aggregates are usually shaped into spherical granules, which are maintained by filamentous cyanobacteria (Takeuchi et al., 2001a, 2001b; Hodson et al., 2010). Filamentous cells of cyanobacteria can entangle mineral and organic particles, and their extracellular polymeric substances (EPS) reinforce these granular forms (Stibal et al., 2012b; Yallop et al., 2012; Musilova et al., 2016). Heterotrophic bacteria, which are sustained by organic matter produced by cyanobacteria and algae, also live within these granules (Margesin et al., 2002). Cyanobacteria mainly colonize the surface of cryoconite granules, whereas heterotrophic bacteria are distributed in the inner part of the granules (Segawa et al., 2020). The formation of microbial aggregates can be beneficial for microbes to resist running water on glacier surfaces. Thus, the formation of cryoconite granules is likely to support the presence of diverse microbes on glaciers.

Phototrophs require nutrients, light, water, and carbon dioxide for their growth. Although light, water, and carbon dioxide are sufficiently available in the supraglacial environment, nutrients such as N and P are often limited and likely to control the growth of phototrophs on the glacial surface. For example, dissolved macronutrients (N and P) in the Greenland ice sheet breed abundant glacial algal communities (Holland et al., 2019); N is primarily supplied to glacial surfaces by wet and dry atmospheric depositions in the form of soluble ions, such as NO_3^- and NH_4^+ (Zhao et al., 2006; Li et al., 2008), whereas, P is supplied in the form of PO_4^{3-} by dissolution from phosphate mineral particles such as apatite, which are deposited on glacial surfaces (Nagatsuka et al., 2010). Because the abundance of these nutrients is often low in the supraglacial environment, limiting microbial growth (Säwström et al., 2007; Stibal et al., 2008a, 2008b; Segawa et al., 2014; Smith et al., 2016).

Mineral dust on the glacier surface also has significant effects on microbes in the supraglacial environment. For example, a significant positive correlation has been recorded between mineral dust and cyanobacteria abundances on a glacier in northwest Greenland (Uetake et al., 2016). As mineral dust can be the substrate of cryoconite granules, abundant mineral dust on the glacial surface could induce the growth of filamentous cyanobacteria. Mineral dust is usually blown by the wind from desert or arid ground surfaces and is deposited and accumulated on glacial surfaces. Because vast deserts extend in the central part of the Eurasian continent, mineral dust is particularly abundant in glaciers of Central Asia (Takeuchi and Li, 2008). The abundant supply of mineral dust on glaciers is likely to cause abundant cryoconite formation, which covers the entire ablating ice surface of glaciers in Central Asia (Takeuchi and Li, 2008). Furthermore, mineral dust is likely to provide P to phototrophs on the glacial surface (Nagatsuka et al., 2010). Glacial algae blooms on the Greenland ice sheet have recently been revealed to be induced by the supply of P in mineral dust (McCutcheon et al., 2021). Mineral dust can also contribute to microbial blooms and further decrease surface albedo.

Although the atmosphere is a major source of soluble nutrients and mineral dust on glacial surfaces, ablating glacier ice can also be a potential source of these substances. Mineral dust and aerosol particles deposited on glacial surfaces in the accumulation area are preserved in glacial ice. Over a long period of time, they move downward with the glacial flow and can finally be released on the glacial surface in the ablation area when the glacial ice melts (Goelles and Bøggild, 2015). A recent study showed that darker ice contained more ancient impurities than brighter ice during the melting season, which was the main reason for the dark zone in the margin of the Greenland ice sheet rather than eolian dust (Wientjes et al., 2012). Ancient ice in Greenland contains richer insoluble impurities as it dates back to the LGM, when the atmospheric dust load was much higher than present (Fuhrer et al., 1999). Several simulations have shown that melt-out dust is the dominant reason for this impurity increase at the ablating glacial ice surface, and the current dust accumulation rates from atmospheric deposition make a minor contribution (Goelles and Bøggild, 2017). Nutrients and mineral dust input from melting surficial ice can be directly measured, or also estimated from ice cores drilled in the ablation area of the considered glaciers. According to this second approach, ice cores can provide the impurity burden of glacial ice, allowing to calculate the potential impurity flux released through ice melting. However, little attention has been paid to their quantitative supply from ablating glacial ice. A few data from the ablation region of glaciers, as most of the attention is paid to the accumulation areas; therefore, their quantitative effects on microbial communities in supraglacial environments remain largely unknown.

Massive glaciers are present above approximately 3,000 m above sea level (a.s.l.) in the Tien Shan Mountains of Central Asia. These glaciers are an important freshwater resource for arid areas (Li et al., 2010). Urumqi Glacier No. 1 is a mountain glacier in this mountain range, located in the headwater of the Urumqi River, which flows down to Urumqi City, inhabited by 3.5 million people. Because of the importance of glaciers as water resource for the local supply, Urumqi Glacier No.1, has been studied as a representative glacier in the river basin for more than 60 years to monitor its mass balance (Xu et al., 2017). These studies have revealed rapid glacial shrinkage over the last 3 decades (Li et al., 2011a). A major reason for this rapid glacial shrinkage is the

increase in the summer air temperature (Zhang et al., 2014). However, albedo reduction by microbes and their products living on the glacial surface also contributes to this rapid glacial decline (Takeuchi and Li, 2008; Takeuchi et al., 2010; Yue et al., 2020). The ablating ice surface of the glacier is densely covered with cryoconite granules consisting of mineral dust and filamentous cyanobacteria (Takeuchi and Li, 2008; Takeuchi et al., 2010). The granular structure of cryoconite has been shown to play an important role in nutrient cycles for microbes, particularly that of N (Segawa et al., 2014; Segawa et al., 2020). The abundant cryoconite on the glacier may have been sustained by nutrient and dust supplies to the supraglacial environment; however, the sources and processes of nutrients and dust on the glacier surface, particularly those from glacial ice, have not been well studied.

This study aims to quantify the concentrations of chemically soluble ions and mineral dust contained in ablating glacial ice, using an ice core drilled from the ablation area of the Urumqi No. 1 Glacier in the Tien Shan Mountains of Central Asia. We estimated the annual fluxes of outcropping solutes and dust from ablation ice and compared them with those from the atmosphere to evaluate the impact of outcropping substances on the supraglacial environment.

2 STUDY SITE AND METHODS

2.1 Study Site

Urumqi Glacier No. 1 (43°06′N, 86°49′E) is in the Tianshan Mountains of the Xinjiang Uygur Autonomous Region in western China. It is a northeast-facing valley glacier ranging from 3,740 to 4,486 m a.s.l. Two branches once flowed together at the terminus of the glacier but were separated into east and west branches in 1993 due to the terminus retreat (Ye et al., 2005). The total area of this glacier is approximately 1.73 km^2. This glacier retreated constantly from 1962 to 2003, with a 20% decrease in the glacier volume (Ye et al., 2005). Glaciers in this region mainly gain mass during summer, when precipitation rates are highest. The mean annual air temperature was −5.0°C, and the mean annual precipitation was 460 mm from 1959 to 2015 in this region, according to records from the Daxigou Meteorological Station (3,593 m a.s.l), located 2 km east of the glacier (Yue et al., 2017). The mean equilibrium line altitude measured from 1997 to 2003 was 4,110 m a.s.l (Ye et al., 2005). The Tianshan Mountains are surrounded by several large deserts, including the Taklimakan to the south, the Gurbantunggut to the north, and the Gobi to the east; thus, dust storms frequently occur in this region (e.g., Li et al., 2010). Dust also carries a wide variety of chemical solutes onto the glacier surface (Dong et al., 2009, 2010, 2011). The ablation area of the glacial surface is covered with abundant cryoconite, with a mean dry weight of 335 g m^{-2} (Takeuchi and Li, 2008). This cryoconite contains mineralogical particles, filamentous and coccoid cyanobacteria, and green algae (Chlorophyta) (Takeuchi et al., 2010), and the mean organic content of the cryoconite was 9.4% (Takeuchi and Li, 2008).

Ice cores have been previously drilled on this glacier, such as the ice core (length: 24.8 m) drilled in the accumulation area at 4,040 m a.s.l in 1998. Ice core analysis have revealed that chemical and isotopic properties vary with depth (Lee et al., 2002) and that anthropogenic pollution alkalizes the glacial surface (Lee et al., 2003). A shallow ice core was drilled again in the accumulation area at 4,130 m a.s.l in 2006. Seasonal variations in mineral dust and organic particles preserved in the ice cores have been described over the past 11 years (Takeuchi et al., 2010). Analysis of the ice core further revealed that abundant microbes grow annually on the snow surface. In 2009, a 56 m ice core was drilled in the ablation area of the glacier, which was used in this study. A shallow ice core drilled in the accumulation area in 2006 was also used to estimate the annual atmospheric deposition of chemical solutes and mineral dust.
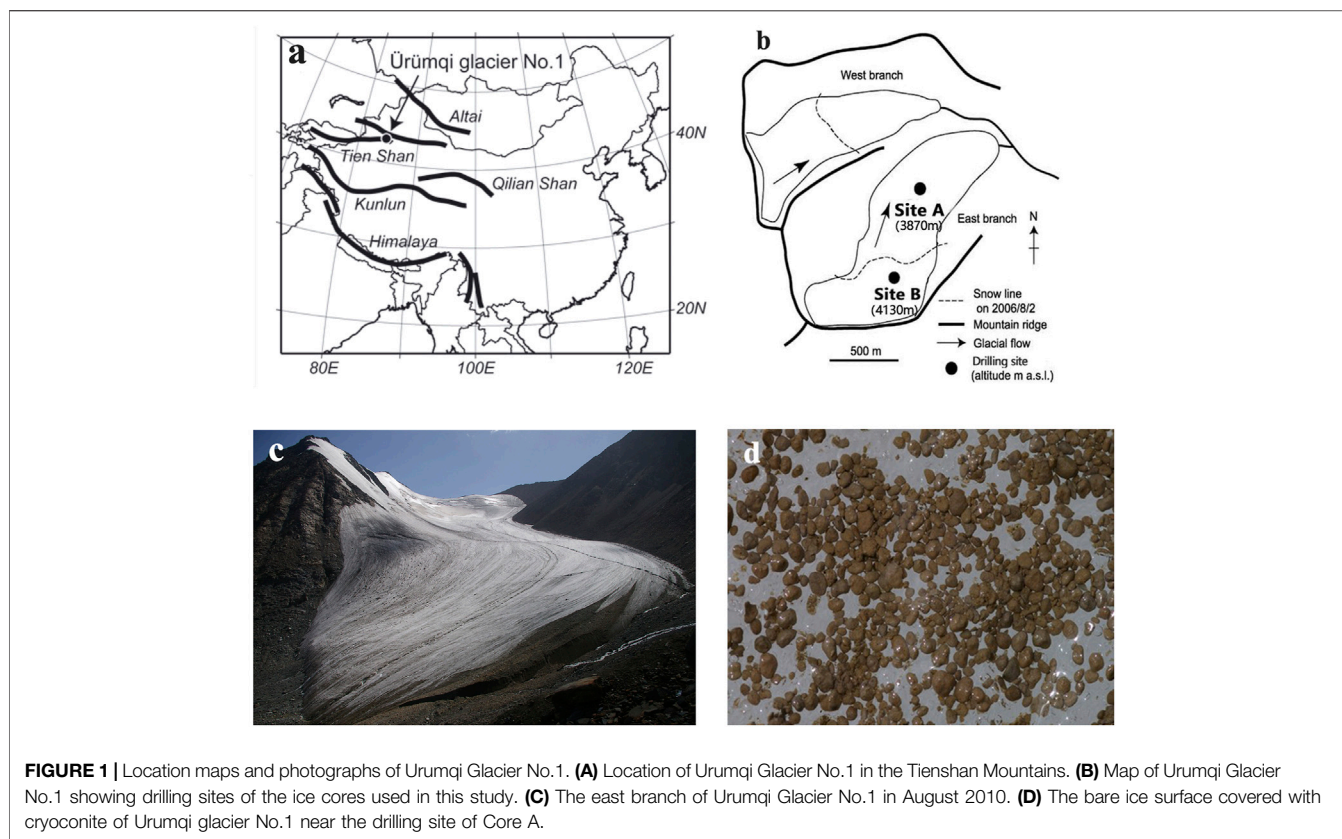
2.2 Methods

2.2.1 Two Ice Cores Analyzed in This Study

The ice core (Core A) analyzed in this study was drilled at 3,870 m a.s.l (Site A, **Figure 1**) in the ablation area of the eastern branch of Urumqi Glacier No. 1 in 2009, at the Tianshan Glaciological Station, Chinese Academy of Sciences. The drilling site was located in the middle of the glacier, away from the margins and the lateral moraines. The total length of the ice core was 55.78 m from the surface to the bedrock of the glacier. The ice core was transported in the frozen state to laboratory of the Cold and Arid Regions Environmental and Engineering Research Institute in Lanzhou, China. The ice core was cut in half lengthwise and transported to Chiba University in Japan in 2011; however, owing to limited transportation capacity, only seven selected parts of the ice core were transported to Japan. In this study, we analyzed these seven sections of the ice core (section 1: 0.00–3.47 m; section 2: 7.52–8.22 m; section 3: 12.04–12.43 m; section 4: 18.94–20.41 m; section 5: 38.02–38.76 m; section 6: 44.54–45.35 m; and section 7: 52.35–55.78 m). The total core length analyzed in this study was 11.01 m.

The seven sections of the ice core were processed for analysis in a low-temperature room (−20°C) at Chiba University in Japan. All sections were cut into samples at 6–9 cm intervals. A total of 161 samples were analyzed. The surfaces of the core samples were scraped off using ceramic knives to eliminate surface contamination. After this treatment, the samples were packed into clean plastic bags (Whirl-pack, United States) and preserved in a low-temperature room until analysis.

To obtain the current supply of aerosols from the atmosphere to the glacier surface, another ice core (Core B) drilled in the accumulation area of the glacier in 2006 (Site B, **Figure 1**) was analyzed. The ice core was drilled at 4,130 m a.s.l in November 2006, from the bottom of a snow pit, from 2.6 m below the surface, down to 7.7 m (total length: 5.1 m). Snow layers above 2.6 m deep were also collected from the snow pit. The stratigraphy, density, and mineral dust concentrations in the core were described by Takeuchi et al. (2010). Oxygen stable isotopes and major chemical solutes of the snow pit and

FIGURE 1 | Location maps and photographs of Urumqi Glacier No.1. **(A)** Location of Urumqi Glacier No.1 in the Tienshan Mountains. **(B)** Map of Urumqi Glacier No.1 showing drilling sites of the ice cores used in this study. **(C)** The east branch of Urumqi Glacier No.1 in August 2010. **(D)** The bare ice surface covered with cryoconite of Urumqi glacier No.1 near the drilling site of Core A.

ice core samples were analyzed in this study. The total number of 123 samples (ice core: 96; snowpit: 27) were analyzed.

2.2.2 Stable Isotope Ratio and Major Ion Concentrations

The ice core samples were melted at room temperature (25 °C) and were filtrated with ion-free filters (Chromate disk, pore size: 0.45 μm, GL Science, Japan) to eliminate insoluble particles before analysis.

Stable isotope ratio of the samples was measured with a liquid-water isotope analyzer (DLT-100, Los Gatos Research, United States) based on cavity ringdown spectroscopy (CRDS) techniques. 1.0 ml of the samples were put into 1.5 ml grass vials (1,030–50,000, GL Sciences, Japan). Three working standards (WS1: −8.35‰, WS2: −14.66‰ and WS3: −9.14‰) were measured before and after every five samples measurement. The δ ^{18}O of the samples was represented by:

$$\delta^{18}O = \left(\frac{R_{sample}}{R_{standard}} - 1 \right) \times 1000 \, (‰)$$

Where R_{sample} is ratio of $^{18}O/^{16}O$ of a sample; $R_{standard}$ is ratio of $^{18}O/^{16}O$ of the standard (V-SMOW). The analytical precision of the δ^{18}O measurements was 0.05 per mill.

Major ionic concentrations, including Cl^-, NO_3^-, and SO_4^{2-} anions, and Na^+, NH_4^+, K^+, Mg^{2+}, and Ca^{2+} cations, were analyzed using an ion chromatography system (ICS-1100, Thermo Fisher, United States).

2.2.3 Mineral Dust Size and Concentration

The mineral dust concentration in each ice core sample was quantified via direct counting using an optical microscope. A volume of 3 ml of the melted sample was put into a 6 ml glass vial and was dried in an oven (60 °C) for 2–3 days until the water of the sample was completely evaporated. To remove organic matter from the samples, 10 ml of hydrogen peroxide solution (30%) was added to the vials, which were placed on a hot plate (80 °C) for 24 h. After the solution was completely dried, 3 ml of Milli-Q water was added to the vials to maintain the original concentration of the mineral dust. The water sample (100 μL) was then filtered through a membrane filter (H020A013A, pore size: 0.2 μm, 13 mm diameter, Ireland). Photographs of the filters containing mineral dust were taken using an optical microscope (BX51, Olympus, Japan). The area of each mineral particle observed in the photographs was automatically measured using an image-processing application (Image-J, National Institutes of Health, United States). The size (diameter) of each particle was calculated from the area as approximate circles by following formula:

$$d = 2\sqrt{\frac{S}{\pi}}$$

Where d is circle diameter, S is circle area.

The number of mineral dust larger than 0.5 μm was then manually counted and the total number of mineral dust particles on the filter was obtained. The mineral dust
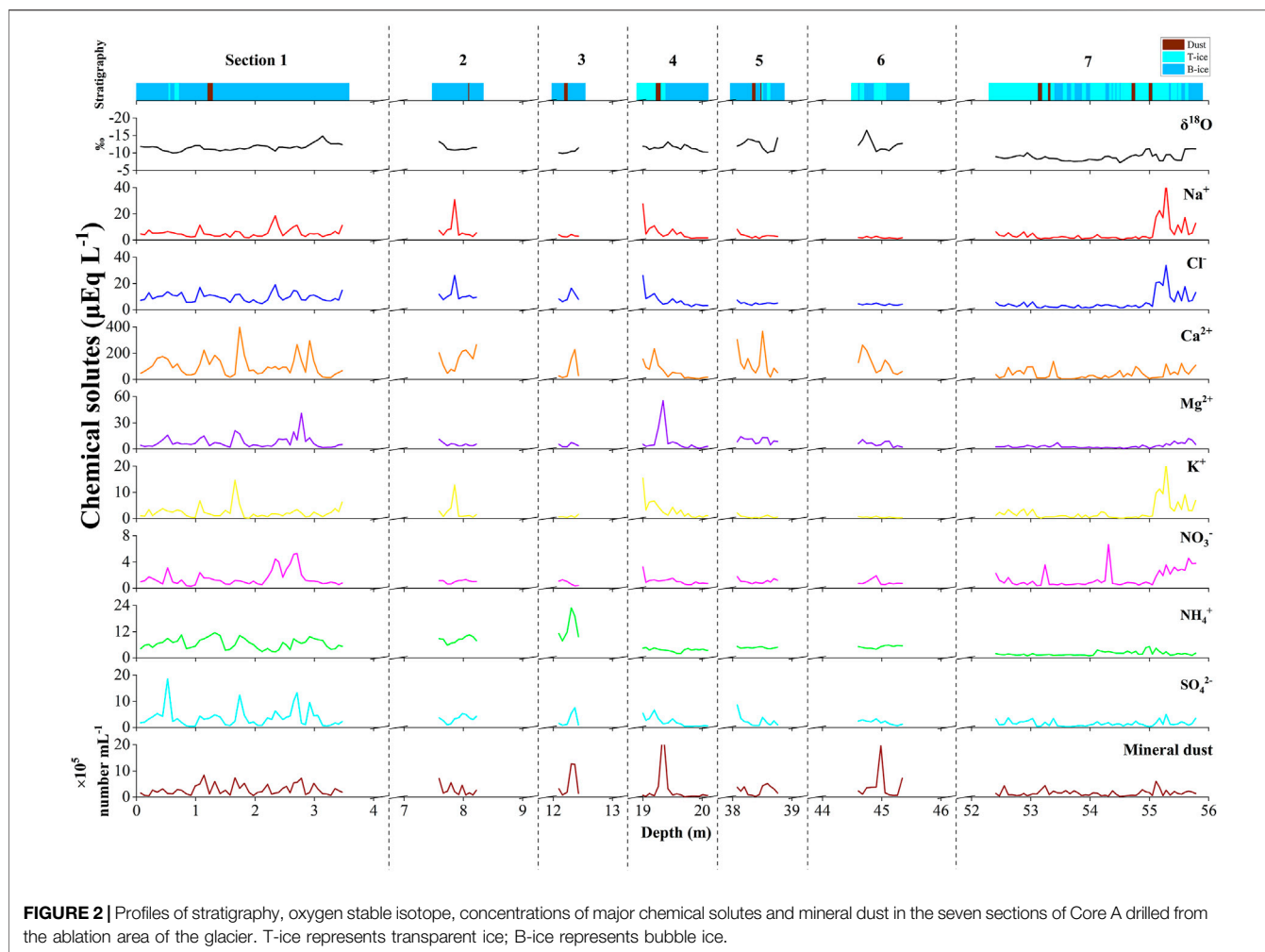
FIGURE 2 | Profiles of stratigraphy, oxygen stable isotope, concentrations of major chemical solutes and mineral dust in the seven sections of Core A drilled from the ablation area of the glacier. T-ice represents transparent ice; B-ice represents bubble ice.

concentration was expressed as the number of dust particles in 1 ml of sample water.

3 RESULTS

3.1 Stratigraphy of the Ice Core

The visual stratigraphy of Core A showed that the seven analyzed sections consisted of ice layers with and without air bubbles (**Figure 2**). There were five prominent dust layers observed visibly at 19.26–19.34 m in section 4, 38.39–38.45 m and 38.51–38.59 m in section 5, and 53.17–53.24 m and 54.77–54.82 m in section 7. Weaker dust layers were also observed at 1.23–1.32 m in section 1, 8.16–8.22 m in section 2, 12.24–12.37 m in section 3, and 53.38–53.45 m and 55.05–55.11 m in section 7.

3.2 Oxygen Stable Isotope

The oxygen stable isotope ratio ($\delta^{18}O$) of the Core A samples ranged from −16.5‰ to −7.2‰ (**Figure 2**). The mean value of all samples in the seven sections was −10.7‰. There were no significant differences in the mean $\delta^{18}O$ values among the upper six sections of the ice core (**Table 1**). However, the mean $\delta^{18}O$ in section 7, which is the deepest part of the ice core, was −8.8‰, which was significantly higher than

those of the other sections. The $\delta^{18}O$ values of the depth profile fluctuates in each section. The $\delta^{18}O$ values in section 1 (3.47 m in length) ranged from −14.8‰ to −10.0‰, including three small peaks. The $\delta^{18}O$ values in section 7 (3.43 m in length) ranged from −11.3‰ to −7.2‰, including five small peaks.

3.3 Major Chemical Soluble Ions

Analysis of the chemical soluble ions in Core A showed that Ca^{2+} was the most dominant ion in all seven sections (**Table 1**; **Figure 2**), ranging from 1.2 to 33.9 µEq L^{-1} (mean: 7.3 µEq L^{-1}). Cl^- was the second dominant ion in the samples, ranging from 4.0 to 397.5 µEq L^{-1} (mean: 79.8 µEq L^{-1}). Mg^{2+}, Na^+, and NH_4^+ were at intermediate levels, while NO_3^-, SO_4^{2-}, and K^+ had relatively lower concentrations. PO_4^{3-} concentrations were under the detection level in all samples (<5 µEq L^{-1}). NO_3^- and NH_4^+ concentrations ranged from 0.3 to 6.7 µEq L^{-1} (mean: 1.3 µEq L^{-1}) and from 0.9 to 22.8 µEq L^{-1} (mean: 4.8 µEq L^{-1}), respectively.

The major soluble ion compositions did not differ significantly among the seven sections (**Figure 3**); however, the mean concentrations of the ions varied slightly among the sections. Cl^-, SO_4^{2-}, and NH_4^+ concentrations were higher in the upper sections (sections 1–3) than in the lower sections (sections 4–7, **Table 1**).

TABLE 1 | Oxygen stable isotope, concentrations of major chemical solutes and mineral dust, and size of minerals in the seven sections of Core A drilled from the ablation area of the glacier.

Section	Depth (m) (length (m))		$\delta^{18}O$ (‰)	Concentration (µEq/L)								Mineral (10^5 num/ml)	Size (µm)
				Na^+	Cl^-	Ca^{2+}	Mg^{2+}	K^+	NO_3^-	NH_4^+	SO_4^{2-}		
1	0.00–3.47 (3.47)	Mean	−11.7	5.6	9.6	100.4	7.7	2.3	1.5	6.5	3.7	2.8	2.6
		Min	−14.8	1.8	4.7	13.3	1.8	0.1	0.3	2.7	0.4	0.5	1.1
		Max	−10.0	18.6	19.1	397.5	41.0	14.7	5.3	11.5	18.5	8.4	58.6
2	7.52–8.22 (0.70)	Mean	−11.4	7.6	11.3	155.5	5.5	2.7	1.0	8.4	3.4	2.7	2.3
		Min	−13.3	2.7	7.7	45.5	3.5	0.5	0.6	5.8	1.0	0.8	1.1
		Max	−10.8	30.8	26.3	264.6	11.1	12.8	1.3	10.5	5.2	7.1	41.5
3	12.04–12.43 (0.39)	Mean	−10.4	3.3	9.8	79.2	4.6	0.8	0.8	13.7	2.9	5.4	2.2
		Min	−11.4	2.4	6.2	45.5	2.5	0.4	0.4	7.7	0.8	0.8	1.1
		Max	−9.9	4.3	16.5	227.6	7.4	1.6	1.3	22.8	7.6	12.7	23.4
4	18.94–20.41 (1.47)	Mean	−11.5	5.1	6.7	51.1	7.8	3.1	1.1	3.7	1.8	2.1	2.6
		Min	−15.0	1.2	2.4	5.2	0.8	0.4	0.5	2.0	0.4	0.2	1.1
		Max	−10.2	27.5	26.1	233.5	55.5	15.4	3.2	4.8	6.6	26.0	50.9
5	38.02–38.76 (0.74)	Mean	−12.4	3.3	4.9	122.9	9.9	0.7	1.0	4.7	2.4	2.6	2.5
		Min	−14.3	1.2	4.3	15.9	4.7	0.2	0.7	4.1	0.8	0.3	1.1
		Max	−10.1	8.1	7.2	367.0	14.2	2.2	1.8	5.2	8.6	5.2	53.5
6	44.54–45.35 (0.81)	Mean	−12.4	1.8	4.0	40.2	5.8	0.5	0.9	5.1	2.0	4.1	1.9
		Min	−16.5	1.0	3.4	4.0	1.5	0.2	0.6	4.0	0.7	0.6	1.1
		Max	−10.4	2.9	5.1	135.8	10.7	0.9	1.9	5.8	3.3	19.6	39.1
7	52.35–55.78 (3.43)	Mean	−8.8	5.0	7.3	40.2	3.2	2.6	1.4	1.9	1.5	1.5	2.5
		Min	−11.3	0.6	1.2	4.0	0.5	0.1	0.4	0.9	0.3	0.3	1.1
		Max	−7.2	42.9	33.9	135.8	12.1	20.7	6.7	5.1	5.0	6.1	55.8
All	(11.01)	Mean	−10.7	5.0	7.3	79.8	6.0	2.2	1.3	4.8	2.5	2.5	2.4

In the uppermost part of the core (section 1), the Ca^{2+} concentration predominantly changed with the depth ranging from 4.0 to 397.5 µEq L^{-1}. Four prominent peaks were observed in this section. Although the Mg^{2+} and SO_4^{2-} concentrations were significantly lower than that of Ca^{2+}, they showed a similar variation to that of Ca^{2+} with four peaks. The Cl^- and Na^+ profiles were similar, but with smaller change amplitudes than that of Ca^{2+}, Mg^{2+}, and SO_4^{2-}. They showed four small peaks in section 1, but the depths of the peaks did not coincide with those of Ca^{2+}, Mg^{2+}, and SO_4^{2-}. The K^+ profile was also different, showing two prominent peaks. The NH_4^+ concentrations fluctuated repeatedly ranging from 2.7 to 11.5 µEq L^{-1} in the section; however, the NO_3^- concentrations were lower but showed two prominent peaks at 2.65 and 2.92 m in this section.

In the deepest part of the ice core (section 7), the concentrations of Ca^{2+}, Mg^{2+}, SO_4^{2-}, and NH_4^+ were generally lower, and the amplitude of their change was also smaller than those in section 1. At the deepest layer, 1 m above the bottom, relatively higher concentrations of Cl^-, Na^+, and K^+ were found. The NO_3^- concentrations were the same level as that in section 1 and showed three peaks (max = 6.7 µEq L^{-1}) in this section.

3.4 Mineral Dust Size and Concentration

The size of mineral dust particles analyzed in the ice core varied from 1.1 to 58.6 µm (mean: 2.4 µm; std = 2.6 µm; n = 24,610; **Table. 1**). There were no significant differences in the size ranges and mean values of the dust particles among the seven sections, although the dust in section 3 was slightly smaller than that from the other sections. Particles between 1 and 4 µm were most dominant with respect to number in all sections, constituting 90.1% of the total amount of mineral dust.

The mineral dust concentrations in the ice core samples ranged from 0.2×10^5 to 26×10^5 number ml^{-1} with a mean of 2.5×10^5 number ml^{-1}. There were no significant differences in mean concentrations among the seven sections. The profile of the dust concentration showed three large peaks in sections 3, 4, and 6 (**Figure 2**), partly corresponding to visible dust layers.

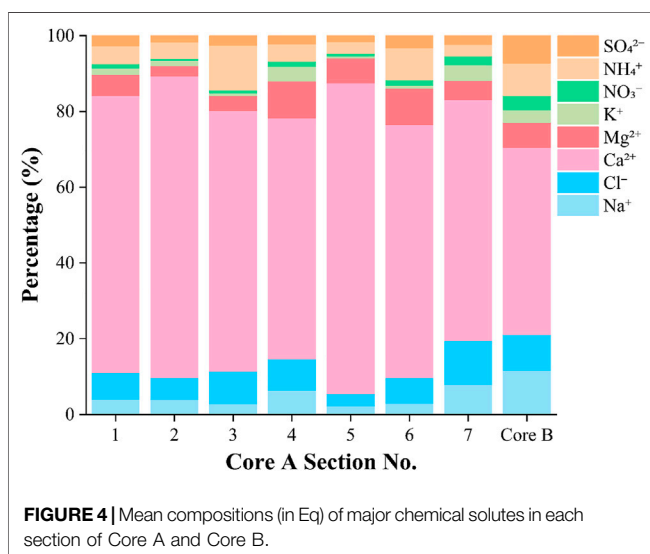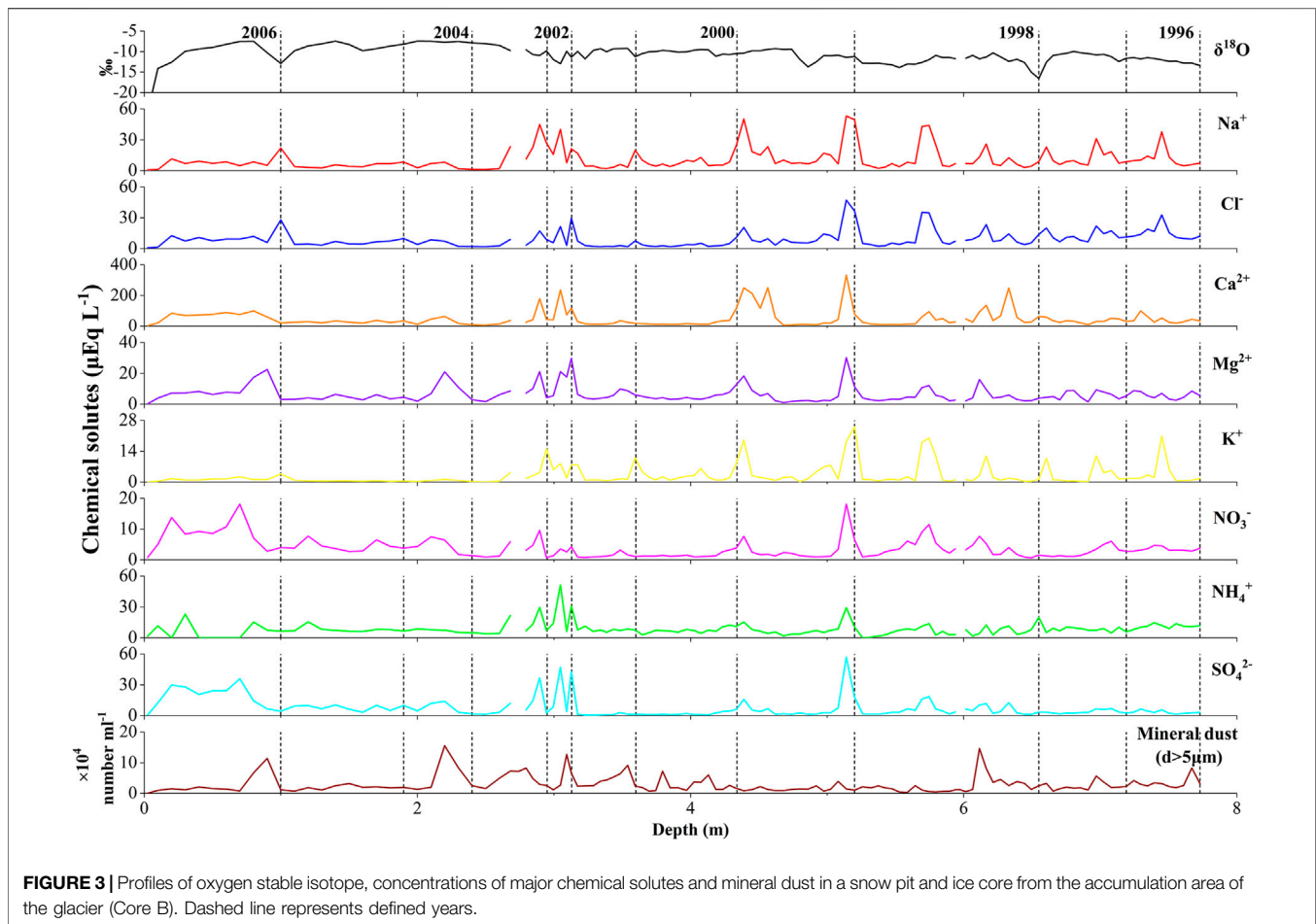## 3.5 Stable Isotope and Chemical Soluble Ions of an Ice Core From the Accumulation Area

The oxygen stable isotopes of the ice core from the accumulation area (Core B) ranged from −24.7‰ to −7.4‰, with a mean of −10.9‰. No clear periodic fluctuations were observed (**Figure 4**).

The major chemical solutes in Core B were also dominated by Ca^{2+}, ranging from 1.8 to 332.7 µEq L^{-1} (mean: 48.5 µEq L^{-1}, **Figures 3, 4**). The concentrations varied with depth, with several peaks from the surface to 7.7 m. The Na^+ levels followed Ca^{2+}, ranging from 0.7 to 53.2 µEq L^{-1}. NO_3^-, in the second-lowest level, was slightly higher than K^+ (3.6 vs. 3.3 µEq L^{-1}), but it had a smaller variation range. The highest concentrations of NH_4^+ and NO_3^- were 51.3 µEq L^{-1}, at 3.02–3.08 m, and 18.2 µEq L^{-1}, at 5.11–5.17 m, respectively.

4 DISCUSSION

4.1 Chemical Characteristics of Glacial Ice in the Ablation Area

As glacial ice in the ablation area of glaciers has moved down from the upper accumulation area over time, ice consisting in

FIGURE 3 | Profiles of oxygen stable isotope, concentrations of major chemical solutes and mineral dust in a snow pit and ice core from the accumulation area of the glacier (Core B). Dashed line represents defined years.

FIGURE 4 | Mean compositions (in Eq) of major chemical solutes in each section of Core A and Core B.

Core A that was analyzed in this study is likely to have formed previously in the accumulation area. In the accumulation area, atmospheric depositions, including chemical solutes and mineral dust on the glacial surface, were preserved annually in snow layers

Although a part of the chemical solutes possibly redistribute across the annual layers by percolating melt water, they are finally buried in glacial ice. They slowly moved down due to glacial flow and reached the lower ablation area of the glacier after substantial time. Thus, the chemical characteristics and mineral dust of glacial ice are likely to reflect past atmospheric depositions. However, the age of the deposition was uncertain, as we did not conduct any absolute dating or chronological analysis in this study.

The mean values of oxygen stable isotope in sections 1 through 6 of Core A (−10.4 to −12.4‰) were almost equivalent to those of Core B (−10.9‰), suggesting that most parts of the Core A were derived from precipitation that occurred in similar climate conditions (i.e., mean air temperature) to the present. Although stable isotope values in Central Asia precipitation can be controlled by several factors, studies have revealed that they are closely correlated with air temperature (Tian et al., 2007). Thus, the similar values of the stable isotope of the glacial ice to those of the present snow (Core B) suggest that most parts of Core A are not as old as the last glacial (possibly having a very low isotope value due to cooler climate) but were probably formed sometime during the Holocene. As the drilling site of Core A was located in the middle of the ablation area of this glacier, this suggests that most of the ice in the ablation area

was formed under similar climate conditions to the present. Contrarily, the mean isotopic value of the bottom part of the ice core (section 7: −8.8‰) was significantly higher than that of the upper sections in Core A. This suggests that the ice near the bottom of the glacier was formed under different climate conditions from that of the other sections. The higher $\delta^{18}O$ value suggests that the ice in section 7 is likely to have formed in a warmer climate than in the present. However, the deepest ice of this glacier is likely to be deformed by glacial flow and thus the original stratigraphic succession of this part is not preserved. Therefore, it is uncertain how glacial ice with high isotope values formed.

There were no significant composition or abundance differences in the chemical characteristics of ice between the ablation and accumulation areas; which indicates that the atmospheric deposition of chemical solutes on the glacier surface did not change significantly from the time of the ice of Core A to the present. Both ice cores from the ablation (Core A) and accumulation areas (Core B) showed the dominance of Ca^{2+}, accounting for more than 50% of the total major solutes analyzed. Although the NO_3^- and NH_4^+ concentrations were generally low in the two cores (<10 µEq L^{-1}), their mean concentrations in Core B were slightly higher than those in Core A (NO_3^-: 3.6 vs. 1.3 µEq/L; NH_4^+: 8.4 vs. 4.8 µEq L^{-1}). NH_4^+ and NO_3^- are considered anthropogenic products, which are likely derived from fossil fuel combustion, biomass burning, livestock manure, and commercial and natural fertilizers (Li et al., 2006). The higher levels of NO_3^- and NH_4^+ in Core B may have been subject to intense human activity in recent years.

4.2 Characteristic of Mineral Dust in the Glacial Ice

Mineral dust particles were observed in all ice core samples from the ablation area (Core A), although only a few dust layers were visible. Comparing Cores A and B, the mean mineral dust concentration (d > 5 µm) was slightly lower in Core A than in Core B (1.9 vs. 2.0 × 10^4 number ml^{-1}), suggesting that atmospheric deposition of mineral dust was less abundant in the past than in the present. However, the presence of mineral dust in Core A ice indicates that the dust particles were supplied not only from the atmosphere but also from glacial ice.

There were no significant differences in the size of mineral dust between Cores A and B, which suggests that the source of dust did not change significantly between the time of Core A and the present. The mineral dust in Cores A and B was dominated by particles smaller than 10 µm but contained particles larger than 50 µm. The size distribution of mineral dust in the ice cores suggests that it was supplied from the ground surface near the glacier and partly from distant deserts. Significant positive correlations between the mineral dust and chemical solute concentrations in the ice core suggest that the dust particles are the source of solutes in the ice. Based on correlation analysis (**Table 2**), the mineral dust concentration was significantly correlated with Mg^{2+} (n = 161, r = 0.58, $p < 0.01$), NH_4^+ (n = 161, r = 0.35, $p < 0.01$), and Ca^{2+} (n = 161, r = 0.23, $p < 0.01$) concentrations. Previous studies have shown that wind-blown

mineral dust combines with and transports various chemical solutes. Ca^{2+} and Mg^{2+} are commonly contained in carbonate minerals; NH_4^+ is usually deposited on glaciers in warm-wet conditions (Li et al., 2008), which partly coincides with seasonal dust occurrence. Therefore, some of the solutes preserved in the ice cores were likely to be supplied by mineral dust.

4.3 Estimation of Annual Fluxes of Outcropping Solutes and Dust From Glacial Ice

The concentrations of chemical solutes and mineral dust in Core A indicate that glacial ice could potentially and continuously affect the supraglacial environment, particularly supraglacial microbes. To understand the significance of how much chemical solutes and mineral dust are supplied by glacial ice, the outcrops of chemical solutes and mineral dust from the glacial ice for a melt season (annual flux) were estimated based on their concentrations and the ice melting rate (unit: m $year^{-1}$) at the drilling site. The concentrations of all chemical solutes and mineral dust fluctuated with depth, indicating that the nutrient and mineral particle supplies from the ice can change as the ice melts. Thus, the mean concentrations were used to estimate the annual material fluxes from glacial ice. The melting rate of the ice surface was obtained by stake measurement of the mass balance observations that ran from September to September of the following year (Li and Zhou, 2011–2016). According to their measurements, the ice surface melting rates at the drilling site between 2007 and 2014 ranged from 0.83 to 2.48 m in water equivalent (w.e.) per year. The mean annual melting of the ice surface in the ablation area of the glacier was 1.56 m w. e., which was used to calculate the annual flux.

The outcrops of each chemical solute from the glacial ice were estimated based on the mean concentrations of each ion analyzed in this study and the annual amount of melt of the glacier surface in w. e. The formula is expressed as follows:

$$Q_i = \mu \times C_i$$

where Q_i represents the annual fluxes of chemical solutes (µEq m^{-2} $year^{-1}$) and µ and C_i represent the annual melting of the ice surface (m^{-3} w. e. $year^{-1}$) and the concentrations of each chemical solute in the glacial ice measured in this study (µEq L^{-1}), respectively. The mean annual fluxes of major chemical solutes (Na^+, Cl^-, Ca^{2+}, Mg^{2+}, NO_3^-, NH_4^+, and SO_4^{2-}) from glacial ice are shown in **Table 3**.

The atmospheric supplies of the chemical solutes were also estimated based on the annual layers and ionic concentrations of Core B. According to Li et al. (2006), chemical solutes at the site of Core B can be redistributed vertically within the snow pack by percolating meltwater during summer. Thus, the concentrations of chemical solutes in the ice core are likely to be altered from the original values of atmospheric depositions and the annual fluxes obtained from the ice core data should not be accurate. However, the chemical solutes can be sequentially incorporated into lower refrozen ice layers if temperatures at the ice layers are sufficiently cold (Li et al., 2006). This observation suggests that the total amounts of ions in the certain range of multi-year snow layers

TABLE 2 | Correlation coefficients between stable isotope, major ions and mineral dust in the ice core collected from the ablation area (Core A).

Elements	$\delta^{18}O$	Na^+	Cl^-	Ca^{2+}	Mg^{2+}	K^+	NO_3^-	NH_4^+	SO_4^{2-}	Mineral
$\delta^{18}O$	-									
Na^+	0.00	-								
Cl^-	−0.18**	0.89**	-							
Ca^{2+}	−0.34**	0.14	0.30**	-						
Mg^{2+}	−0.26**	0.07	0.15	0.35**	-					
K^+	0.03	0.86**	0.79**	0.05	0.13	-				
NO_3^-	0.01	0.47**	0.45**	0.12	0.21	0.34**	-			
NH_4^+	−0.40**	0.00	0.39**	0.50**	0.19*	−0.06	−0.06	-		
SO_4^{2-}	−0.17*	0.33**	0.49**	0.71	0.29**	0.21**	0.43**	0.45**	-	
Mineral	−0.13	0.03	0.14	0.23**	0.59**	0.04	0.03	0.35**	0.19*	-

*Note: ** denotes p < 0.01; * denotes p < 0.05.*

TABLE 3 | Annual fluxes of chemical solutes and mineral dust (d > 5 µm) from the atmosphere and from the glacial ice estimated by ice cores analyzed in this study.

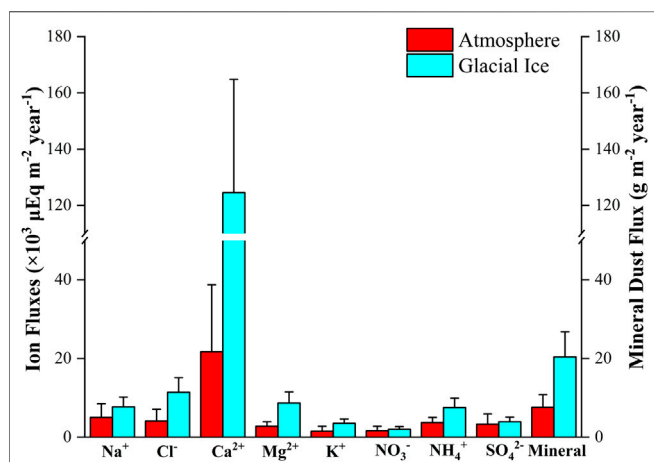|		Na^+	Cl^-	Ca^{2+}	Mg^{2+}	K^+	NO_3^-	NH_4^+	SO_4^{2-}	Mineral Dust
					$\times 10^3$ µEq m^{-2} year^{-1}					g m^{-2} year^{-1}
From atmosphere	Mean	5.0	4.1	21.7	2.8	1.5	1.6	3.7	3.3	7.6
(Core B)	SD	3.5	3.0	17.0	1.1	1.3	1.2	1.3	2.6	3.2
From glacial ice	Mean	7.7	11.4	124.5	8.7	3.5	2.0	7.5	3.9	20.4
(Core A)	SD	2.5	3.7	40.3	2.8	1.1	0.7	2.4	1.2	6.4

SD denote standard deviation.

FIGURE 5 | Annual fluxes of chemical solutes and mineral dust (d > 5 µm) from the atmosphere and from the glacial ice estimated by ice cores analyzed in this study.

was preserved in the firn and refrozen ice although the amounts of ions deposited at each annual layer were altered. Therefore, the mean annual ion fluxes obtained from the 11 years record of Core B was used to compare those from glacial ice in this study.

The mean ion fluxes (Na^+, Cl^-, Ca^{2+}, Mg^{2+}, NO_3^-, NH_4^+, and SO_4^{2-}) from the atmosphere are shown in **Figure 5**. For fluxes from both glacial ice and the atmosphere, Ca^{2+} was dominant among the major solutes. The mean annual fluxes of NO_3^- and SO_4^{2-} from the atmosphere and glacial ice are almost equivalent. This indicates that the quantity of chemical solutes is determined

not only by their concentrations in the ice but also by the annual melting rate. The concentrations and fluxes of NH_4^+ from the atmosphere were both slightly higher than those from the glacial ice. Therefore, glacial ice could play a major role in supplying N for microbes, although the supply from glacial ice largely depends on the annual amount of ice melting. Additionally, glacial ice is likely to play a more significant role in supplying nutrients to microbes on the glacier surface.

The outcropping mineral dust from glacial ice was similarly estimated. The mineral dust flux was represented as the total mass of the mineral particles. The mass of the single mineral particles was determined by the density of a typical atmospheric mineral particle (approximately 2,500 kg m^{-3}) (Steffensen, 1997), and the geometric volume of a particle was assumed to be a sphere. The formula for calculating mineral flux is expressed as follows:

$$Q_i = m \times \mu \times C_i$$

where Q_i (g m^{-2} year^{-1}) represents the annual fluxes of mass of outcropping mineral dust from the glacier surface and m, µ, and C_i represent the mean mass of a single mineral particle (g), the annual amount of melt of the glacier surface (m^{-3} w. e. year^{-1}), and the mean concentration of mineral particles (number ml^{-1}) obtained in this study, respectively. Consequently, the mean annual mass flux of mineral dust from glacial ice was calculated as 20.4 g m^{-2} year^{-1}.

We also estimated the annual flux of atmospheric supply of mineral dust using Core B. The mineral dust concentration of Core B was quantified by Takeuchi et al. (2010), but the range of particle sizes analyzed was different. Therefore, we used the concentrations of the dust particles larger than 5 µm. The annual flux of mineral dust from the atmosphere obtained from the Core B ranged from 4.3

to 15.9 g m^{-2} year^{-1}, with an average of 7.6 g m^{-2} year^{-1}. This mean annual flux was approximately one-third of the outcropping mineral dust from glacial ice obtained in this study (**Figure 5**; **Table 3**), suggesting that outcropping mineral dust from glacial ice is a major source of mineral dust on the glacial surface.

4.4 Effect of Glacial Ice on Supraglacial Ecosystems

Our results showed that chemical solutes and mineral dust outcroppings from glacial ice were likely to significantly affect the supraglacial environment of the glacier. Particularly, the fluxes of chemical solutes of N may affect microbial abundances or community structures on the glacier because N is an essential element for microbial growth on the glacier surface (Telling et al., 2011). Recent studies have revealed that specific microbes within cryoconite granules drive nitrogen cycles on this glacier surface (Segawa et al., 2014; 2020). Nitrogen fixation, nitrification, and denitrification occur in cryoconite granules under size-dependent conditions. N is mostly assimilated by cyanobacteria in small granules. In large-sized granules, cyanobacteria are only active at the surface of the granules, and nitrification and denitrification occur in the inner part of the granules. Another important nutrient for supraglacial microbes is P (Cook et al., 2016); however, phosphate (PO$_4^{3-}$) was not detected in either of the ice cores in this study, suggesting that its supply as a soluble ion was limited to this glacier. Studies have reported that P is supplied to glaciers in the form of mineral dust (apatite). Some mineral dust can be biologically weathered by microbes, and P in the dust can be assimilated by microbes (Zawieruch et al., 2019). Sr stable isotope ratio analysis of cryoconite also suggest that microbes incorporate nutrients from phosphate minerals (apatite) and other saline and carbonate minerals (Nagatsuka et al., 2010). Therefore, the outcropping of mineral dust from glacial ice may support the supply of P to microbes in the supraglacial environment of this glacier.

The significant supply of outcropping mineral dust from glacial ice is likely necessary for the abundant presence of cryoconite on the surface of Urumqi Glacier No. 1. Cyanobacteria, the dominant microbes on glacial surfaces (Segawa et al., 2014), form cryoconite granules (Takeuchi et al., 2010). The granules grow annually during the melt season, entangled with mineral dust and other particles, as shown by microscopic observations of the cross-section of the granules (Takeuchi et al., 2010). As cyanobacteria prefer alkaline aquatic conditions, carbonates contained in the mineral dust, which could change the meltwater alkaline, may support cyanobacterial growth. A study on Greenlandic glaciers revealed that mineral dust abundances were the main factors affecting cyanobacterial growth (Uetake et al., 2016). Mineral dust particles may act as the bases of filamentous cyanobacteria during the early stage of granule formation because free microbial cells are easily washed out by running meltwater (Uetake et al., 2016). Size of mineral particles within cryoconite granules on this glacier were reported to be between 1.3 and 98 μm in diameter, (Takeuchi et al., 2010), which roughly corresponds to the size range of mineral dust in the ice cores in this study. Therefore, the supply of mineral dust from glacial ice, in addition to atmospheric supply, can facilitate the formation of cryoconite granules.

Our study was based on a single ice core from the glacier ablation area. The melt rate of the ice surface varied largely among the observational years and sites of this glacier (Li and Zhou, 2011–2016). Because the outcropping of the material from the ice is largely dependent on the melt rate of the glacier surface, the fluxes of substances from the glacial ice obtained in this study may spatially vary within the glacier. Furthermore, all substances are unlikely to be incorporated by microbes because the supraglacial environment is not static. Most substances may be hydrologically washed out of the glacier by running surface meltwater. As we did not measure the fluxes of the substances running out of the glacier, it is uncertain how much of the outcropping substances were incorporated by microbes on the glacier surface. It is important to quantify the budgets of nutrients and mineral dust to better understand glacial ecosystems.

Despite such uncertainties, our study showed that the outcropping solute and mineral dust supplies are comparable to or greater than those of atmospheric supplies to supraglacial environments. Although atmospheric nutrient and mineral dust supplies have been considered to be the only source of microbes on the glacier (Ren et al., 2019), our results clearly showed that glacial ice plays a significant role in supraglacial environments and that the greater melting of glacial ice changes the chemical conditions and increases the microbial supply of nutrients on the ablating ice surface. Owing to recent climate warming, an increase in the melt rate has been reported on this glacier (Zhang et al., 2014). A higher melt rate of the ablation surface causes more materials to be outcropped from glacial ice, which are released onto the glacier surface. Such an increase in material flux might cause changes in the abundance of microbes on the glacier surface. Therefore, further studies to evaluate outcropping substances from glacial ice are necessary.

5 CONCLUSION

The characteristics of the major chemical solutes and mineral dust in an ice core drilled from the ablation area of Urumqi Glacier No. 1 in the Tien Shan Mountains were analyzed. The most dominant ion in the ice core was Ca^{2+}, followed by Cl$^-$, SO$_4^{2-}$, NH$_4^+$, and NO$_3^-$. The mean dust concentration in the ice core was 2.5 ×10^5 number ml^{-1}. Additionally, the concentrations of soluble chemical ions and mineral dust vary with depth in the ice core. They are likely to have been derived from previous atmospheric depositions, likely during the Holocene. The mean chemical solute and mineral dust concentrations were compared with those from another ice core collected from the accumulation area of the glacier. There were no significant differences in chemical composition, mineral size, and ionic and mineral concentrations between the two ice cores, suggesting that atmospheric depositions of chemical solutes and mineral dust on the glacier surface did not significantly change from the time of ice formation in the ablation area to the present. Based on these results, the annual fluxes of the major soluble ions and mineral dust outcropping from the ablating glacial ice were estimated using the observational melt rate at the ice surface. The results showed that the fluxes of chemical solutes and mineral dust from the ablating ice were comparable to or higher than those deposited from the atmosphere. This indicates that glacial ice is a major source of chemical solutes and mineral dust on glacial surfaces.

Our results revealed that melting glacial ice supplies chemical solutes and mineral dust to the supraglacial environment and that the change in the melting rate of glacial ice would affect the chemical conditions and the growth of photoautotrophs on the ablating ice surface, although it is necessary to further investigate the quantitative impact of the outcropping materials on glacial microbes.

DATA AVAILABILITY STATEMENT

The raw data supporting the conclusion of this article will be made available by the authors, without undue reservation.

AUTHOR CONTRIBUTIONS

YC and NT designed research. FW and ZL conducted the ice core drillings and physical analyses of the ice cores. YC and NT analyzed stable isotope ratio, soluble ions, and mineral dust in the samples. YC and NT wrote the manuscript.

FUNDING

ACKNOWLEDGMENTS

REFERENCES

Barry, R. G. (2006). The Status of Research on Glaciers and Global Glacier Recession: a Review. *Prog. Phys. Geogr. Earth Environ.* 30 (3), 285–306. doi:10.1191/0309133306pp478ra

Bøggild, C. E., Brandt, R. E., Brown, K. J., and Warren, S. G. (2010). The Ablation Zone in Northeast Greenland: Ice Types, Albedos and Impurities. *J. Glaciol.* 56, 101–113. doi:10.3189/002214310791190776

Bond, T. C., Doherty, S. J., Fahey, D. W., Forster, P. M., Berntsen, T., DeAngelo, B. J., et al. (2013). Bounding the Role of Black Carbon in the Climate System: A Scientific Assessment. *J. Geophys. Res. Atmos.* 118, 5380–5552. doi:10.1002/jgrd.50171

Cook, J., Edwards, A., Takeuchi, N., and Irvine-Fynn, T. (2016). Cryoconite: The Dark Biological Secret of the Cryosphere. *Prog. Phys. Geogr. Earth Environ.* 40 (1), 66–111. doi:10.1177/0309133315616574

Dong, Z., Li, Z., Edwards, R., Wu, L., and Zhou, P. (2011). Temporal Characteristics of Mineral Dust Particles in Precipitation of Urumqi River Valley in Tian Shan, China: a Comparison of Alpine Site and Rural Site. *Atmos. Res.* 101 (1-2), 294–306. doi:10.1016/j.atmosres10.1016/j.atmosres.2011.03.002

Dong, Z., Li, Z., Wang, F., and Zhang, M. (2009). Characteristics of Atmospheric Dust Deposition in Snow on the Glaciers of the Eastern Tien Shan, China. *J. Glaciol.* 55 (193), 797–804. doi:10.3189/002214309790152393

Dong, Z., Li, Z., Xiao, C., Wang, F., and Zhang, M. (2010). Characteristics of Aerosol Dust in Fresh Snow in the Asian Dust and Non-dust Periods at Urumqi Glacier No. 1 of Eastern Tian Shan, China. *Environ. Earth Sci.* 60 (7), 1361–1368. doi:10.1007/s12665-009-0271-6.28

Fuhrer, K., Wolff, E. W., and Johnsen, S. J. (1999). Timescales for Dust Variability in the Greenland Ice Core Project (GRIP) Ice Core in the Last 100,000 Years. *J. Geophys. Res.* 104 (D24), 31043–31052. doi:10.1029/1999JD900929

Goelles, T., and Bøggild, C. E. (2015). Albedo Reduction Caused by Black Carbon and Dust Accumulation: a Quantive Model Applied to the Western Margin of the Greenland Ice Sheet. *Cryosphere Discuss.* 9 (1), 1345–1381. doi:10.5194/tcd-9-1345-2015

Goelles, T., and Bøggild, C. E. (2017). Albedo Reduction of Ice Caused by Dust and Black Carbon Accumulation: a Model Applied to the K-Transect, West Greenland. *J. Glaciol.* 63 (242), 1063–1076. doi:10.1017/jog.2017.74

Haeberli, W., Cihlar, J., and Barry, R. G. (2000). Glacier Monitoring within the Global Climate Observing System. *Ann. Glaciol.* 31, 241–246. doi:10.3189/172756400781820192

Hodson, A., Cameron, K., Bøggild, C., Irvine-Fynn, T., Langford, H., Pearce, D., et al. (2010). The Structure, Biological Activity and Biogeochemistry of Cryoconite Aggregates upon an Arctic Valley Glacier: Longyearbreen, Svalbard. *J. Glaciol.* 56 (196), 349–362. doi:10.3189/002214310791968403

Hoham, R. W., and Remias, D. (2020). Snow and Glacial Algae: A Review1. *J. Phycol.* 56 (2), 264–282. doi:10.1111/jpy.12952

Holland, A. T., Williamson, C. J., Sgouridis, F., Tedstone, A. J., McCutcheon, J., Cook, J. M. E., et al. (2019). The Black and Bloom GroupDissolved Organic Nutrients Dominate Melting Surface Ice of the Dark Zone (Greenland Ice Sheet). *Biogeosciences* 16, 3283–3296. doi:10.5194/bg-16-3283-2019

Huilin, L., Zhongqin, L., Wenbin, W., and Feiteng, W. (2008). Depositional Characteristics of NH_4^+ on Ürümqi Glacier No. 1, Eastern Tien Shan, China. *Ann. Glaciol.* 49, 161–165. doi:10.3189/172756408787814762

Langford, H., Hodson, A., Banwart, S., and Bøggild, C. (2010). The Microstructure and Biogeochemistry of Arctic Cryoconite Granules. *Ann. Glaciol.* 51 (56), 87–94. doi:10.3189/172756411795932083

Lee, X., Qin, D., Jiang, G., Duan, K., and Zhou, H. (2003). Atmospheric Pollution of a Remote Area of Tianshan Mountain: Ice Core Record. *J. Geophys. Res.* 108 (D14), 181. doi:10.1029/2002JD002181

Li, Z., Edwards, R., Mosley-Thompson, E., Wang, F., Dong, Z., You, X., et al. (2006). Seasonal Variability of Ionic Concentrations in Surface Snow and Elution Processes in Snow-Firn Packs at the PGPI Site on Ürümqi Glacier No. 1, Eastern Tien Shan, China. *Ann. Glaciol.* 43, 250–256. doi:10.3189/172756406781812069

Li, Z., He, Y., An, W., Song, L., Zhang, W., Catto, N., et al. (2011b). Climate and Glacier Change in Southwestern China during the Past Several Decades. *Environ. Res. Lett.* 6, 045404. doi:10.1088/1748-9326/6/4/045404

Li, Z., Li, H., and Chen, Y. (2011a). Mechanisms and Simulation of Accelerated Shrinkage of Continental Glaciers: a Case Study of Urumqi Glacier No. 1 in Eastern Tianshan, Central Asia. *J. Earth Sci.* 22 (4), 423–430. doi:10.1007/s12583-011-0194-5

Li, Z., Wang, W., Zhang, M., Wang, F., and Li, H. (2009). Observed Changes in Streamflow at the Headwaters of the Urumqi River, Eastern Tianshan, Central Asia. *Hydrol. Process.* 24 (2), a–n. doi:10.1002/hyp.7431

Li, Z., and Zhou, P. (2011-2016). *Annual Report of Tienshan Glaciological Station*. Lanzhou, China: Cold and Arid Regions Environmental and Engineering Research Institution, Chinese Academy of Sciences. 19-23.

Margesin, R., Zacke, G., and Schinner, F. (2002). Characterization of Heterotrophic Microorganisms in Alpine Glacier Cryoconite. *Arct. Antarct. Alp. Res.* 34 (1), 88–93. doi:10.1080/15230430.2002.12003472

McCutcheon, J., Lutz, S., Williamson, C., Cook, J. M., Tedstone, A. J., Vanderstraeten, A., et al. (2021). Mineral Phosphorus Drives Glacier Algal Blooms on the Greenland Ice Sheet. *Nat. Commun.* 12 (1), 1–11. doi:10.1038/s41467-020-20627-w

Musilova, M., Tranter, M., Bamber, J. L., Takeuchi, N., and Anesio, A. (2016). Experimental Evidence that Microbial Activity Lowers the Albedo of Glaciers. *Geochem. Persp. Let.* 2, 106–116. doi:10.7185/geochemlet.1611

Nagatsuka, N., Takeuchi, N., Nakano, T., Kokado, E., and Li, Z. (2010). Sr, Nd and Pb Stable Isotopes of Surface Dust on Ürümqi Glacier No. 1 in Western China. *Ann. Glaciol.* 51 (56), 95–105. doi:10.3189/172756411795931895

Ren, Z., Martyniuk, N., Oleksy, I. A., Swain, A., and Hotaling, S. (2019). Ecological Stoichiometry of the Mountain Cryosphere. *Front. Ecol. Evol.* 7. doi:10.3389/fevo.2019.00360

Säwström, C., Laybourn-Parry, J., Granéli, W., and Anesio, A. M. (2007). Heterotrophic Bacterial and Viral Dynamics in Arctic Freshwaters: Results from a Field Study and Nutrient-Temperature Manipulation Experiments. *Polar Biol.* 30 (11), 1407–1415. doi:10.1007/s00300-007-0301-3

Segawa, T., Ishii, S., Ohte, N., Akiyoshi, A., Yamada, A., Maruyama, F., et al. (2014). The Nitrogen Cycle in Cryoconites: Naturally Occurring Nitrification-Denitrification Granules on a Glacierfication-Denitrification Granules on a Glacier. *Environ. Microbiol.* 16 (10), 3250–3262. doi:10.1111/1462-2920.12543

Segawa, T., Takeuchi, N., Mori, H., Rathnayake, R. M. L. D., Li, Z., Akiyoshi, A., et al. (2020). Redox Stratification within Cryoconite Granules Influences the Nitrogen Cycle on Glaciers. *FEMS Microbiol. Ecol.* 96 (11), fiaa199. doi:10.1093/femsec/fiaa199

Smith, H. J., Schmit, A., Foster, R., Littman, S., Kuypers, M. M., and Foreman, C. M. (2016). Biofilms on Glacial Surfaces: Hotspots for Biological Activity. *npj Biofilms Microbiomes* 2 (1), 1–4. doi:10.1038/npjbiofilms.2016.8

Steffensen, J. P. (1997). The Size Distribution of Microparticles from Selected Segments of the Greenland Ice Core Project Ice Core Representing Different Climatic Periods. *J. Geophys. Res.* 102 (C12), 26755–26763. doi:10.1029/97JC01490

Stibal, M., Telling, J., Cook, J., Mak, K. M., Hodson, A., and Anesio, A. M. (2012b). Environmental Controls on Microbial Abundance and Activity on the Greenland Ice Sheet: a Multivariate Analysis Approach. *Microb. Ecol.* 63, 74–84. doi:10.1007/s00248-011-9935-3

Stibal, M., Tranter, M., Benning, L. G., and ehk, J. (2008a). Microbial Primary Production on an Arctic Glacier Is Insignificant in Comparison with Allochthonous Organic Carbon Input. *Environ. Microbiol.* 10 (8), 2172–2178. doi:10.1111/j.1462-2920.2008.01620.x

Stibal, M., Tranter, M., Telling, J., and Benning, L. G. (2008b). Speciation, Phase Association and Potential Bioavailability of Phosphorus on a Svalbard Glacier. *Biogeochemistry* 90 (1), 1–13. doi:10.1007/s10533-008-9226-3

Takeuchi, N., Fujita, K., Aizen, V. B., Narama, C., Yokoyama, Y., Okamoto, S., et al. (2006). A Snow Algal Community on Akkem Glacier in the Russian Altai mountainsThe Disappearance of Glaciers in the Tien Shan Mountains in Central Asia at the End of Pleistocene. *Ann. Glaciol. Sci. Rev.* 43103, 37826–38433. doi:10.1016/j.quascirev.2014.09.006

Takeuchi, N., Ishida, Y., Kubota, K., Takeuchi, N., Ishida, Y., Li, Z., et al. (2011b). Microscopic Analyses of Insoluble Particles in an Ice Core of Ürümqi Glacier No. 1: Quantification of Mineral and Organic particlesMicroscopic Analysis of Insoluble Particles in an Ice Core of Ürümqi Glacier No. 1: Quantification of Mineral and Organic Particles. *J. Earth Sci.* 1822 (4), 65431–69440. doi:10.1007/s12583-011-0197-2

Takeuchi, N., Kohshima, S., and Seko, K. (2001a). Structure, Formation, and Darkening Process of Albedo-Reducing Material (Cryoconite) on a Himalayan Glacier: a Granular Algal Mat Growing on the Glacier. *Arct. Antarct. Alp. Res.* 33 (2), 115–122. doi:10.1080/15230430.2001.12003413

Takeuchi, N., and Li, Z. (2008). Characteristics of Surface Dust on Ürümqi Glacier No. 1 in the Tien Shan Mountains, China. *Arct. Antarct. Alp. Res.* 40 (4), 744–750. doi:10.1657/1523-0430(07-094)[takeuchi]2.0.co;2

Takeuchi, N., Matsuda, Y., Sakai, A., and Fujita, K. (2005). A Large Amount of Biogenic Surface Dust (Cryoconite) on a Glacier in the Qilian Mountains, China. *Bull. Glaciol. Res.* 22, 1

Takeuchi, N., Nishiyama, H., and Li, Z. (2010). Structure and Formation Process of Cryoconite Granules on Ürümqi Glacier No. 1 , Tien Shan, China. *Ann. Glaciol.* 51 (56), 9–14. doi:10.3189/172756411795932010

Takeuchi, N. (2002). Optical Characteristics of Cryoconite (Surface Dust) on Glaciers: the Relationship between Light Absorbency and the Property of Organic Matter Contained in the Cryoconite. *Ann. Glaciol.* 34, 409–414. doi:10.3189/172756402781817743

Telling, J., Anesio, A. M., Tranter, M., Irvine-Fynn, T., Hodson, A., Butler, C., et al. (2011). Nitrogen Fixation on Arctic Glaciers, Svalbard. *J. Geophys. Res.* 116 (G3), 1632. doi:10.1029/2010JG001632

Tian, L., Yao, T., MacClune, K., White, J. W. C., Schilla, A., Vaughn, B., et al. (2007). Stable Isotopic Variations in West China: A Consideration of Moisture Sources. *J. Geophys. Res.* 112 (D10), 7718. doi:10.1029/2006JD007718

Uetake, J., Tanaka, S., Segawa, T., Takeuchi, N., Nagatsuka, N., Motoyama, H., et al. (2016). Microbial Community Variation in Cryoconite Granules on Qaanaaq Glacier, NW Greenland. *FEMS Microbiol. Ecol.* 92 (9), fiw127–10. doi:10.1093/femsec/fiw127

Wientjes, I. G. M., Van De Wal, R. S. W., Schwikowski, M., Zapf, A., Fahrni, S., and Wacker, L. (2012). Carbonaceous Particles Reveal that Late Holocene Dust Causes the Dark Region in the Western Ablation Zone of the Greenland Ice Sheet. *J. Glaciol.* 58 (210), 787–794. doi:10.3189/2012JoG11J165

Wiscombe, W. J., and Warren, S. G. (1980). A Model for the Spectral Albedo of Snow. I: Pure Snow. *J. Atmos. Sci.* 37 (12), 2712–2733. doi:10.1175/1520-0469(1980)037<2712:amftsa>2.0.co;2

Xinqing, L., Dahe, Q., Shugui, H., Jiawen, R., Keqin, D., and Hui, Z. (2002). Changes in Chemical and Isotopic Properties Near Infiltrated Cracks in an Ice Core from Ürümqi Glacier No. 1, Tien Shan, China. *Ann. Glaciol.* 35, 162–166. doi:10.3189/172756402781816762

Xu, C., Li, Z., Wang, F., Li, H., Wang, W., and Wang, L. (2017). Using an Ultra-long-range Terrestrial Laser Scanner to Monitor the Net Mass Balance of Urumqi Glacier No. 1, Eastern Tien Shan, China, at the Monthly Scale. *J. Glaciol.* 63 (241), 792–802. doi:10.1017/jog.2017.45

Yallop, M. L., Anesio, A. M., Perkins, R. G., Cook, J., Telling, J., Fagan, D., et al. (2012). Photophysiology and Albedo-Changing Potential of the Ice Algal Community on the Surface of the Greenland Ice Sheet. *Isme J.* 6, 2302–2313. doi:10.1038/ismej.2012.107

Ye, B., Yang, D., Jiao, K., Han, T., Jin, Z., Yang, H., et al. (2005). The Urumqi River Source Glacier No. 1, Tianshan, China: Changes over the Past 45 Years. *Geophys. Res. Lett.* 32 (21), L21504. doi:10.1029/2005GL024178

Yue, X., Li, Z., Zhao, J., Fan, J., Takeuchi, N., and Wang, L. (2020). Variation in Albedo and its Relationship with Surface Dust at Urumqi Glacier No. 1 in Tien Shan, China. *Front. Earth Sci.* 8, 110. doi:10.3389/feart.2020.00110

Yue, X., Zhao, J., Li, Z., Zhang, M., Fan, J., Wang, L., et al. (2017). Spatial and Temporal Variations of the Surface Albedo and Other Factors Influencing Urumqi Glacier No. 1 in Tien Shan, China. *J. Glaciol.* 63 (241), 899–911. doi:10.1017/jog.2017.57

Zawierucha, K., Baccolo, G., Di Mauro, B., Nawrot, A., Szczuciński, W., and Kalińska, E. (2019). Micromorphological Features of Mineral Matter from Cryoconite Holes on Arctic (Svalbard) and Alpine (The Alps, the Caucasus) Glaciers. *Polar Sci.* 22, 100482. doi:10.1016/j.polar.2019.100482

Zawierucha, K., Kolicka, M., Takeuchi, N., and Kaczmarek, Ł. (2015). What Animals Can Live in Cryoconite Holes? A Faunal Review. *J. Zool.* 295 (3), 159–169. doi:10.1111/jzo.12195

Zawierucha, K., Porazinska, D. L., Ficetola, G. F., Ambrosini, R., Baccolo, G., Buda, J., et al. (2021). A Hole in the Nematosphere: Tardigrades and Rotifers Dominate the Cryoconite Hole Environment, whereas Nematodes Are Missing. *J. Zool.* 313 (1), 18–36. doi:10.1111/jzo.12832

Zhang, G., Li, Z., Wang, W., and Wang, W. (2014). Rapid Decrease of Observed Mass Balance in the Urumqi Glacier No. 1, Tianshan Mountains, Central Asia. *Quat. Int.* 349, 135–141. doi:10.1016/j.quaint.2013.08.035

Zhao, Z., Li, Z., Edwards, R., Wang, F., Li, H., and Zhu, Y. (2006). Atmosphere-to-snow-to-firn Transfer of NO_3^- on Ürümqi Glacier No. 1, Eastern Tien Shan, China. *Ann. Glaciol.* 43, 239–244. doi:10.3189/172756406781812410